Entrainment Rates and Eddy Exchange Coefficients from Reanalysis Sea Surface Salinity Data

Nathan Paldor[1], Ofer Shamir[1,2], Itamar Yacoby[1]

[1]Fredy and Nadine Herrmann Institute of Earth Sciences, Hebrew University of Jerusalem, Jerusalem, Israel
[2]Present Affiliation: Courant Institute of Mathematical Sciences, New York University, NYC, NY, USA

Key Points:

- In some oceanic circumstances, changes in Sea Surface Salinity gradient provide a simple, reliable and robust diagnostic of ocean currents
- Changes in the entrainment rate of surrounding water into a current, correspond to observable changes in Sea Surface Salinity gradient
- Reanalysis Sea Surface Salinity data quantify the ratio between the speed of advection and the eddy exchange coefficient in slow currents

Corresponding author: Nathan Paldor, `nathan.paldor@mail.huji.ac.il`

Abstract

Simple analytic models developed in this study are applied to long-term averages of re-analysis surface salinity data to quantify two fundamental properties of ocean currents. The first model is based on the new Freshening Length schema and its application to the Irminger Current yields a ratio of about 5 between the turbulent entrainment rates of surrounding fresher surface waters west and east of Greenland. The second model is based on the steady solution of the advection-diffusion equation subject to suitable boundary conditions. The application of this model to the spreading of fresh, snow-melt, water from the delta of the Po river in the northwest Adriatic Sea into the rest of the Sea yields a ratio of $8{\times}10^4$ m between the eddy exchange coefficient and the speed of advection in the Sea.

Plain Language Summary

Differences in ocean water salinity were used for over a century to quantify the horizontal fluxes in and out of evaporative, motionless, basins such as the Mediterranean Sea. In the present study we develop simple expressions based on analytic models that extend the century-old approach to ocean currents where the water is constantly moving rather than remaining stagnant. The models developed here are combined with long-term data of sea surface salinity along two currents – the salty Irminger Current that flows around the southern tip of Greenland and the flow of fresh snow-melt water from the Po river into the Adriatic Sea. The models and climatological data used here yield quantitative estimates of two basic parameters: A) The rate at which a high-salinity current detrains salt to the surrounding ocean. B) The balance between the slow downstream advection and eddy (turbulent) exchange coefficient. The models developed in this study can be applied to other currents and regions of the world ocean.

1 Introduction

In 1900 the Danish oceanographer Martin Knudsen developed a model that relates vertical salinity variations to the exchange of water between a river and the adjacent estuary (an English translation of Knudsen's work, published originally in German, can be found in Burchard et al., 2018). In the 120 years that elapsed from its development the model has become textbook material (e.g. Knauss & Garfield, 2016) and was extensively used for estimating the horizontal transports in and out of semi-enclosed basins such as the Mediterranean sea (e.g. Bryden & Kinder, 1991), the Red sea (e.g. Sofianos & Johns, 2002) and the Gulf of Elat (e.g. Paldor & Anati, 1979; Wolf-Vecht et al., 1992). In these applications transports in and out of a basin are required to balance the excess of evaporation over precipitation (including river run-off) in the basin. The controlling parameter in these applications is the difference between the Sea Surface Salinity (SSS hereafter) and the salinity of a deeper layer where the presumed return flow out of the basin takes place.

More sophisticated and detailed applications of the Eulerian form of the conservation of salt and water were subsequently developed using salinity coordinates. This approach examines the conservation of salt and water in a closed sub-domain bounded on one of its sides by a (curved) isohaline. Two oceanic circumstances in which the application of this idea proved fruitful include the vertical and horizontal mixing of river plumes in estuaries (e.g. Hetland, 2005, 2010) and the decadal changes that occur in the two-layer exchange between two intermediate size seas – the Baltic Sea and the North Sea (Burchard et al., 2018).

A Lagrangian variant of Knudsen's model is the Evaporation Length schema, developed in Berman et al. (2019). This schema focuses on the horizontal change in SSS that occurs due to net evaporation, q, (i.e. evaporation minus total fresh water influx) in a column of water that flows in a current that extends between the ocean surface ($z = 0$) and a constant depth $z = -h$. The schema utilizes the change in salinity along the current to calculate a parameter termed Evaporation Length defined by

$$L = \frac{S}{\frac{\partial S}{\partial x}}. \tag{1}$$

Here, $\frac{\partial S}{\partial x}$ is the salinity gradient along the current and $S \gg \Delta S$ (where $\Delta S = \int \frac{\partial S}{\partial x} dx$ is the total change in salinity along the current) is the current's initial/mean salinity. L is the hypothetical length that the column can travel before all its water evaporates completely. In this, Evaporation Length, schema qL (where L is determined from the SSS distribution) equals the current's volume transport (per unit length in the cross-stream direction) Uh (where U is the mean current's speed) i.e.

$$qL = Uh. \tag{2}$$

The Evaporation Length schema can be generalized to circumstances where a salty current flows in a sea of fresher water and entrains the surrounding fresher waters along its path. This scenario typifies the Irminger Current that flows around Greenland in the Irminger and Labrador seas (see the current denoted by the red line in Figure 1a). In this case the salinity decreases along the current due to eddy exchange with the surrounding ocean on the sides of the current and not due to removal of pure water at the surface by evaporation. The corresponding L in this scenario is called the Freshening Length. At Cape Farewell (the southern tip of Greenland) the salty Irminger Current undergoes qualitative changes. First, west of Cape Farewell the Current flows much closer to the Greenland coast than east of it (see e.g. Figure 9 in Pickart et al., 2003). Second, west of Greenland and due to the intense cooling, the high-salinity water transported by the Current sinks to the deep ocean to close the thermohaline circulations cell (see e.g. Drinkwater et al., 2020) while east of Greenland the Current flows horizontally with little or no interruptions. The Freshening Length schema, developed in the next section, mandates that these qualitative changes should be reflected in different SSS distributions along the Current east and west of Greenland.

A different scenario typifies the long-term averaged SSS distribution in the Adriatic Sea shown in Figure 1b. Here, the SSS distribution clearly shows a small, low salinity, region at the westernmost segment of the Adriatic Sea near its north coast. The low salinity in this region results from the fresh water flow into the Sea by the Po river that empties snow-melt water in a delta located about 50 km south of Venice. The spreading of the low-salinity water from this source region to the rest of the Sea involves advection and eddy (turbulent) exchange associated with the unique general circulation of the Adriatic Sea. In the 20^{th} century (see e.g. Artegiani et al., 1997; Poulain, 1999) the general circulation in the Sea was shown to consist of 3 main gyres aligned along the Sea's NW-SE axis and a number of smaller scale gyres, most of which are seasonal. These features of the general circulation are also found in recent studies such as Oddo and Guarnieri (2011). Though the speed of the currents at the perimeters of the gyres exceeds 0.3 ms^{-1} (Poulain, 1999) the net speed of fresh water flux in the Sea (i.e. away from the delta of the Po river) is very small and cannot be directly measured. The analyses described in (Falco et al., 2000) confirm that velocity estimates based on drifter tracking are subject to large errors and a few drifters even propagate northwestwards. The conclusion is that while the SSS data clearly shows a net flux of fresh water from the head of the Sea to its mouth, direct observations of this flow do not provide a reliable estimate. This uncertainty in the magnitude of the mean flow is probably due to the strong eddy turbulent exchange associated with the gyres that dominates the general circulation in the Sea that masks the small mean flow.

Both the Freshening Length schema and point-source model listed above employ salinity fields which are routinely stored in all climatological model and data archives. The present study proposes that the long-term averaged distributions of SSS in clima-

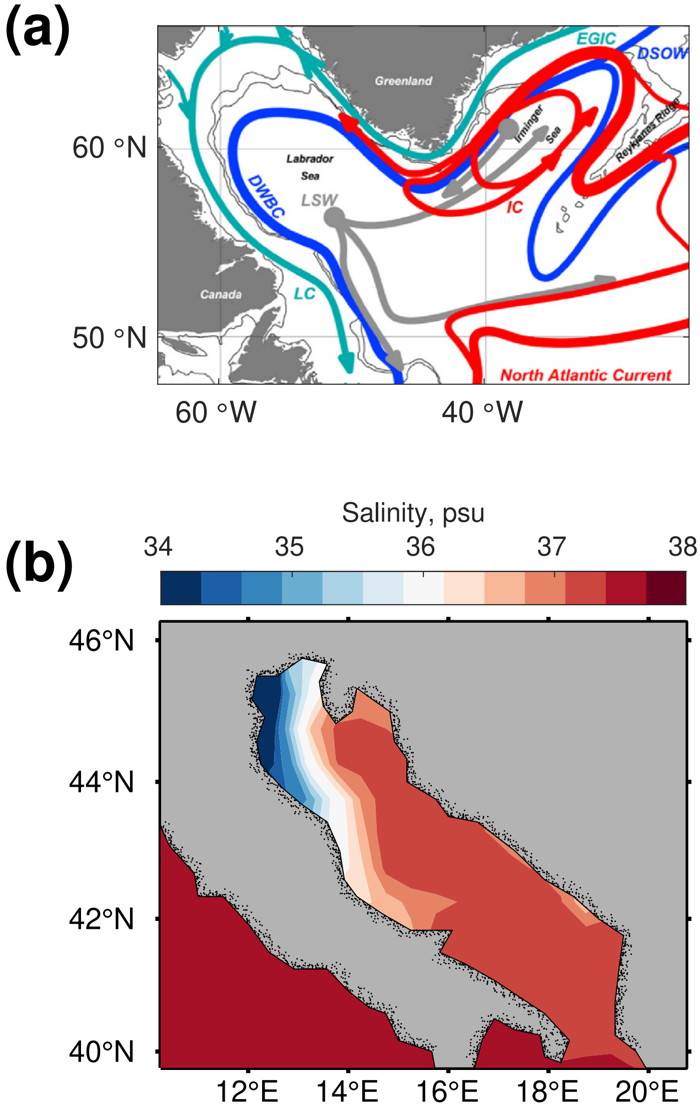

Figure 1. (a) The Irminger Current (red curve) carries high salinity water (that originates in the North Atlantic Current) poleward. The Current follows a complicated path with a couple of North/South turns caused by the vorticity constraints imposed by the Reykjanes Ridge south of Iceland. Near the southern tip of Greenland the Current flows southwestward east of Greenland (in the Irminger sea) and northwestward (in the Labrador sea). Adapted with permission from Little et al. (2019). (b) The Sea Surface Salinity distribution in the Adriatic Sea calculated by averaging 37-year of SODA surface salinity values.

tological, reanalysis, data archives can be employed to characterize and quantify the difference in the rates of entrainment in the two limbs of the Irminger Current. The SSS from the same data archive is also used to quantify the relative roles of mean flow versus that of eddy exchange in the Adriatic Sea. In both cases the existing velocity data do not provide direct estimates of the entrainment rates in the Irminger Current and transports in the Adriatic Sea since velocity cannot be simply related to entrainment rate in the former and since the sought mean velocity is highly uncertain (because it is a small residual of large northward and southward directed velocities) in the latter. This study demonstrates that salinity reanalysis data can be reliably used to estimate the entrainment rate and eddy exchange coefficient. The reanalysis data source, the methods employed in analysing the data and the development of the two mathematical models that employ these data are described in Sec. 2. In Secs. 3 and 4 the two models are applied to the SSS reanalysis data to characterize properties of the two flows. The paper ends with a summary and discussion in Sec. 5.

2 Data, Methods and the Theoretical Models

The data used in this study are all taken from the "Simple Ocean Data Assimilation" or SODA project. Technical details of these data are given in Carton et al. (2018) and the data can be freely accessed at https://rda.ucar.edu/datasets/ds650.0/. The spatial resolution of the gridded data assimilation product is 0.5 degrees in latitude and longitude and the temporal resolution is 5 days. Time series of salinity, temperature and velocity data span the period of nearly 37 years from January 3, 1980 to December 19, 2017. The uppermost point (surface) in the data archive is located at a depth of 5m and all data used here represent averages over the entire 37 years. Salinity data were employed in both applications described in sections 3 and 4 while temperature and velocity data were used in the Freshening Length application described in section 3. The SSS fields are employed in both models described in the following subsections.

(a) The Freshening Length schema is developed here and applied to the Irminger Current. The geographical region of interest here is 45°W and 35°W between 55°N and 65°N, i.e. the seas near the southern part of Greenland. The first step in the analysis was to determine, at each latitude, the first longitudes of maximum salinity east and west of Greenland (i.e. the two maxima closest to the coasts of Greenland). The Irminger Current was then identified by the 5-point zonal average (about 100 km at these latitudes) centered on the local salinity maximum and the process was repeated at every latitude along the Irminger Current. Downstream transects of surface salinity and temperature east and west of Cape Farewell were calculated from the zonal and temporal averages of SODA data. The distance x along the transects was calculated as the spherical geodesic distance between maximal salinity points i.e. ∂x in salinity gradient term (see e.g. equation (1)) is the geodesic distance between two adjacent salinity maxima. The two panels of Figure 2 show the locations of the zonal salinity maxima to the east (blue symbols) and west (red symbols) between Cape Farewell and 63.75°N along with the contours of salinity (panel a) and temperature (panel b). The Irminger Current is identified in all subsequent salinity, temperature and velocity (i.e. flux or transport) calculations by the local maximum in surface salinity.

The Freshening Length schema is developed here for a high-salinity current that flows in a low-salinity ambient ocean. The turbulent exchange of water with the ambient ocean along the current's sides causes the salinity to decrease along the current. The physical scenario is depicted in Figure 3 where a current of high salinity S_1 flows in an ambient ocean of lower salinity $S_0 < S_1$. The arrows across the sides of the current denote turbulent (horizontal) mixing that causes the entrainment of surrounding, low salinity, water into the current and the detrainment of same volume of salty Irminger Current water out of it. The global map of net surface water flux (i.e. evaporation - precipitation) in (Schmitt, 1995) shows negligible fluxes, which cannot be reliably distinguished

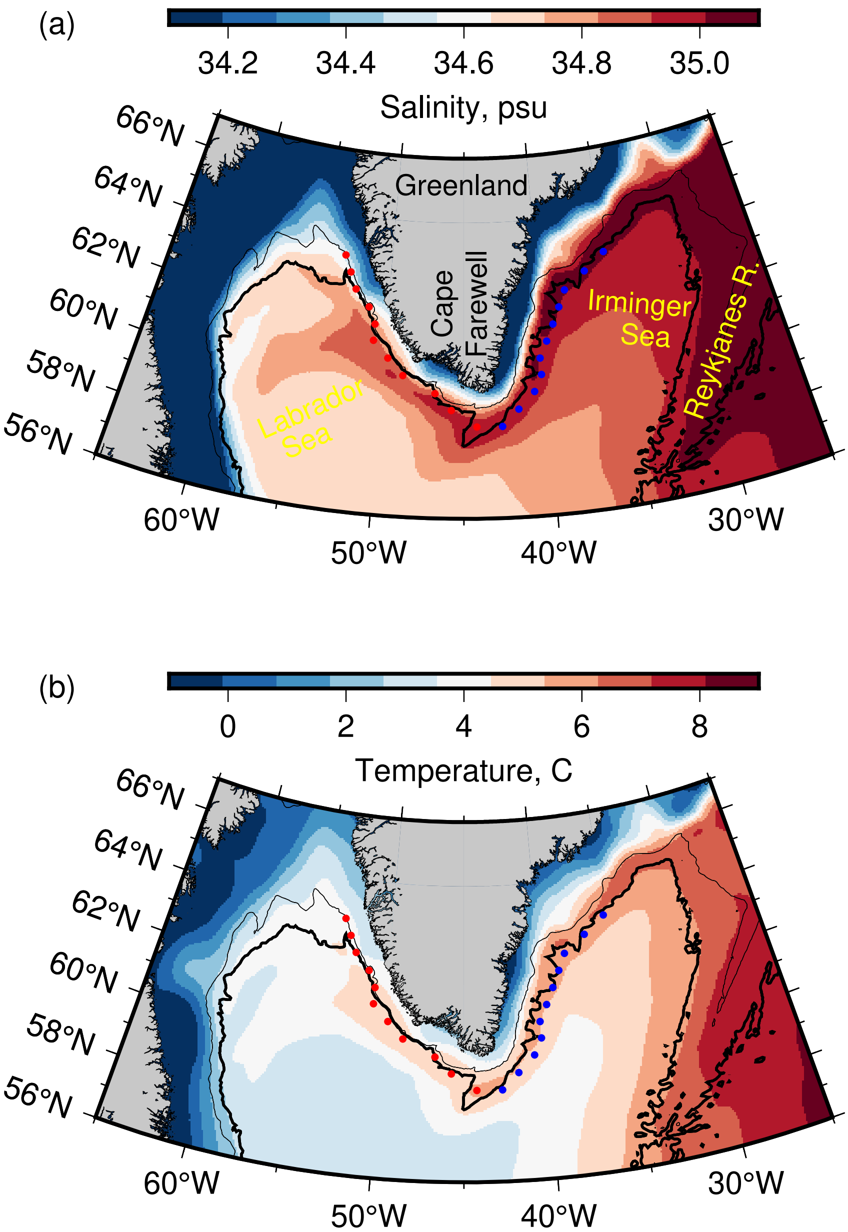

Figure 2. 37-year averages of surface salinity in psu (a) and temperature in °C (b) around southern Greenland. Blue and red filled circles indicate the location of surface salinity maxima along constant longitudes east and west of Greenland, respectively. Black contours are 1000 m and 2000 m bottom depths.

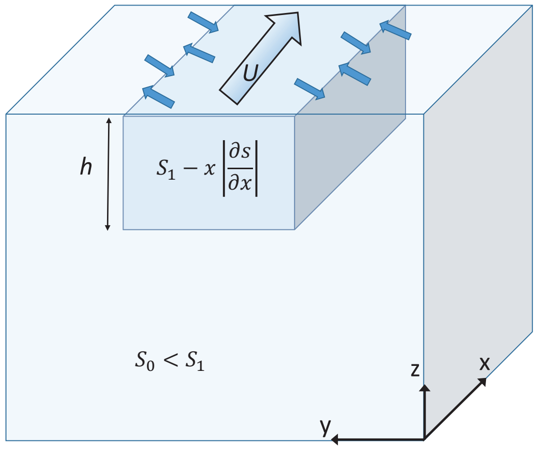

Figure 3. A high salinity current flowing in a surrounding low-salinity ocean entrains the low-salinity water due to turbulent mixing between the current and the surrounding ocean. The entrainment of low salinity water along its flow causes the salinity of the current itself to decrease with downstream distance.

from zero, in the sub-polar North Atlantic (mainly due to the low water vapour content in the atmosphere) so changes in the Current's salinity originate mainly from the horizontal exchange with the surrounding ocean. The salinity S_1 is the average salinity across the Current's width at a particular depth at $x = 0$. The downstream change in salinity, $x\frac{\partial S}{\partial x}$, is assumed much smaller than either S_0 or S_1 at all x. Consider a strip of unit length along the current and width W across the current. If the eddy volume exchange of water per unit area is k (units: ms^{-1}) then over a time interval Δt, the mass of salt removed from the current to the surrounding ocean – M_s (note: $M_s < 0$) along the 2 sides of the strip (of depth h) is

$$M_s = 2k\rho h(S_0 - S_1)\Delta t. \tag{3}$$

Letting $\Delta t = x/U$ (where U is the mean speed of the current) and relating M_s to the change in the salinity of the strip at point x, ΔS, via $M_s = \Delta S \rho W h$ yields:

$$\frac{\Delta S}{S_0 - S_1} = \frac{x}{L} \tag{4}$$

where $L = \frac{WU}{2k}$ is the Freshening Length. However, in contrast to the Evaporation Length, here L quantifies the distance that the strip has to travel for its salinity to fully change from S_1 to S_0. The term $\frac{\Delta S}{x}$ in equation (4) is approximated by $\frac{\partial S}{\partial x}$, the salinity gradient along the current, so this equation implies

$$L = \frac{S_0 - S_1}{\frac{\partial S}{\partial x}} \tag{5}$$

i.e. $L \propto (\frac{\partial S}{\partial x})^{-1}$ as in the Evaporation Length schema. The definition $q = 2k$ transforms the $L = \frac{UW}{2k}$ relation to a form similar to equation (2):

$$qL = UW = F, \tag{6}$$

where F is the current's volume transport per unit height.

(b) Point-source model quantifies the spatial distribution of surface salinity in the Adriatic Sea. The SSS distribution shown in panel b of Figure 1 suggests that since the

Po river empties into the Sea on its north-west coast, the primary salinity variation along the Sea takes place in the zonal direction whereas in the meridional direction the salinity is nearly uniform. Accordingly, the salinity value at any particular longitude along the center-line of the Sea was determined by averaging the salinity values along all latitudes within the Adriatic Sea at that particular longitude.

The $E-P$ flux across the surface is much smaller than either E or P so its sign cannot be reliably estimated from observations. This near balancing of E and P is evident in the data given in Table 3 of Artegiani et al. (1997) which clearly shows that the main source of salinity variation along the Sea is the fresh water flux. The analysis of Raicich (1996) attributes nearly all of the fresh water inflow into the Adriatic Sea to snow melting from the Dynaric Alps and the Apennines that empties into the Sea at its north-west corner via the Po river.

Accordingly, with the 0.5° resolution of SODA data, the fresh water inflow into the Adriatic Sea via the Po river is considered a point source of low-salinity water. After leaving the mouth of the Po river the low-salinity water is incorporated into the general circulation in the Sea that, according to e.g Poulain (2001), consists of 3 main gyres aligned along the axis of the sea and additional short-lived, smaller, gyres located mainly near the coasts. The speed at the gyres' perimeters exceeds 0.3 ms^{-1} but the analyses in Notarstefano et al. (2008) demonstrate that the averaged (in time and cross-sea direction) downstream speeds do not exceed 0.02 ms^{-1}. Thus, the steady model employed here for describing the flow of fresh water from the head of the Sea in the northwest to Otranto strait in the southeast consists of a slow propagation speed, U and turbulent exchange driven by the gyral flow. Thus, we assume that the distribution of salinity along the sea, $S(x)$, (where x is the distance from the head of the Sea) satisfies the steady one-dimensional advection-diffusion equation:

$$0 = U\frac{\partial S}{\partial x} + \kappa \frac{\partial^2 S}{\partial x^2}, \tag{7}$$

where κ (units: $m^2 s^{-1}$) is the turbulent eddy exchange coefficient. The solution of this equation that satisfies the boundary conditions $S(x = 0) = S_0$ and $S(x = x_{end}) = S_{end}$ (where x_{end} denotes the Strait of Otranto) is:

$$S(x) = S_0 + (S_{end} - S_0)\frac{1-\exp\left(-\frac{U}{\kappa}x\right)}{1-\exp\left(-\frac{U}{\kappa}x_{end}\right)} \approx S_{end} - (S_{end} - S_0)\exp\left(-\frac{U}{\kappa}x\right). \tag{8}$$

The last expression in (8) provides an accurate approximation provided $\frac{U}{\kappa}x_{end} \gg 1$ i.e. when $S(x)$ is nearly constant at $x < x_{end}$. Though this equation is a trivial solution of the steady advection-diffusion equation with appropriate boundary conditions, its application to a slow, basin wide, flow using reanalysis SSS data is new.

Having developed the two models we turn now to their application to the SSS distributions in the two regions. In particular, we wish to estimate the values of q (the entrainment rates) in the two limbs of the Irminger Current from equation (6) and the value of U/κ in the Adriatic Sea from equation (8).

3 The Freshening Length Schema in the Irminger Current

The distributions of SSS (panel a) and temperature (panel b) in Figure 2 were calculated from averages of SODA data between the Reykjanes Ridge in the east and Labrador in the west. The Reykjanes Ridge to the south of Iceland is part of the Mid-Atlantic Ridge system where salinities and temperatures at the surface generally exceed 35 psu and 8°C, respectively. The climatological cyclonic mean circulation in the Irminger Sea distributes warm and salty Irminger surface water preferentially near the 2000-m isobath in agreement with the modern mooring observations of de Jong et al. (2012). This figure also

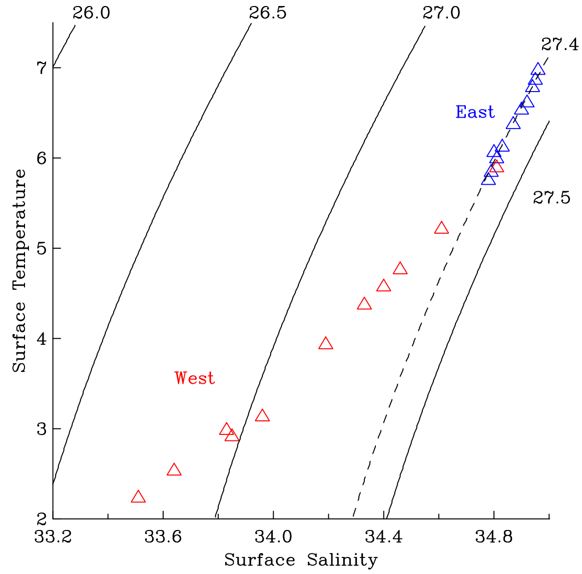

Figure 4. Surface temperature-salinity diagram (triangular symbols) over density contours (solid and dashed thin lines) for the stations shown in Figure 2 and used in Figure 5. Red and blue triangles denote stations along the western and eastern limbs, respectively.

shows that much fresher water occupies the continental shelf and slope regions off Greenland delineated by the 1000-m isobath to the east of 55° W longitude. The surface water of the Irminger Current wraps around Cape Farewell and extends northward into the Labrador Sea. Along its path, however, it freshens and cools as it mixes with the fresh and cold surrounding waters.

The T-S diagrams of surface waters shown in Figure 4 clearly indicate that different mixing regimes prevail east and west of Greenland. The data from the eastern limb of the Irminger Current (shown by blue triangles) all fall closely on a density contour of 1027.4 Kg$\cdot$ m^{-3}. In contrast, the data from the western limb (shown by red triangles) follow a nearly straight line that crosses density contours between 1027.4 and 1026.6 Kg $\cdot$m^{-3} (for location of points see Figure 2). While the T-S diagram clearly indicates that different mixing processes act in the two limbs, it provides no quantitative information on the rate at which the salty water of the Irminger Current freshens as it entrains the fresher ambient water along its flow. In contrast, the Freshening Length schema can quantify the ratio between the entrainment rates in the two limbs.

Figure 5 shows the surface salinity variations along the Irminger current east (panel b) and west of Greenland (panel a). Geographically, the curves in the two panels are continued from the right bottom corner of panel (b) to the upper left corner of panel (a). Figure 5 shows the $S(x)$ distributions in the Irminger Current east (right panel) and west (left panel) of Greenland along with the corresponding least square linear approximations. The slopes of the least square approximations, -0.0016 and -0.00030, yield a ratio of $L_{east}/L_{west} = \left(\frac{\partial S}{\partial x}\right)_{west}/\left(\frac{\partial S}{\partial x}\right)_{east} = 5.5$ between the Freshening Lengths in the two limbs of the Current. The correlated variance R^2 of salinity and distance along the transect east and west of Greenland are 0.92 and 0.97, respectively. Notice that the eastern transect starts at 63.75N and extends to the south-west, while the western transect starts at 58.75N and extends to the north-west to the same 63.75N latitude.

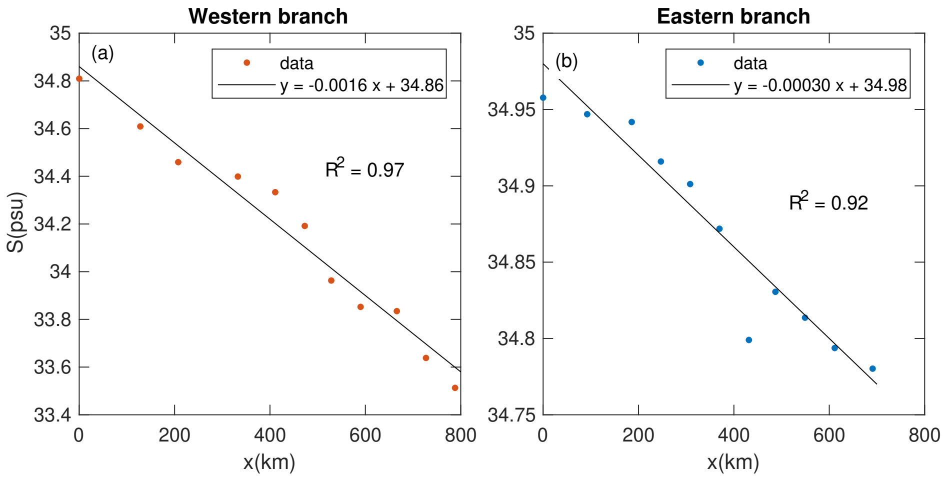

Figure 5. Salinity (psu) along the points of maximal values in Figure 2. The salinity in each limb is averaged over the 5 grid points containing the maximum and two adjacent grid points on either sides of the maximum. x is the spherical geodesic distance along the trajectory, i.e. Δx is the geodesic distance between two adjacent maxima. The slopes and intercepts of the least square linear fit lines are noted in each panel

The entrainment rates into the Irminger Current's east and west limbs, can be quantified by rewriting Equation (6) as $q = F/L$ and combining the calculated values L with direct estimates of the surface fluxes – F.

The first step in the estimation of F is the determination of the observed downstream surface velocity, V (not to be confused with the model downstream surface velocity U). Two methods are employed to estimate V in the 2 limbs of the Irminger Current. In the first method we assume that V is given by $V = \sqrt{u^2 + v^2}$ where u and v are SODA's zonal and meridional surface velocities, respectively. This method assumes that the cross-stream velocity is negligible. In the second method of calculating V, we project SODA's velocity vector $u\hat{i}+v\hat{j}$, where $\hat{i}$ and $\hat{j}$ are unit vectors in the zonal and meridional directions respectively, onto the downstream direction of the current in the 2 limbs. These mean downstream directions are oriented at azimuths of about 220° (eastern limb) and 310° (western limb). Following the calculation of the downstream velocities, V, by the two methods at all points within the current, the downstream averaged values were determined by averaging the values of V over the 10 downstream values (grid points). Next, the downstream averages are averaged once again over the 5 cross-stream grid points. These downstream and cross-stream averaged values of V are then multiplied by the width of the current, W, to estimate the transport (per unit height) – F.

The transports in the two limbs calculated from the averaged values of V are shown in Table 1 for the two methods of calculating V. Clearly, the ratio between the fluxes in the two limbs is $F_{east}/F_{west} \sim 1.2$ in both methods used of calculating V.

Having determined the ratio between the values of L and F, the ratio between the values of $q = F/L$ in the Current's east and west limbs is readily determined from Equation (6) as:

$$\frac{q_{east}}{q_{west}} = \frac{(F/L)_{east}}{(F/L)_{west}} = \frac{F_{east}/F_{west}}{L_{east}/L_{west}} \approx 1.2/5.5 = 0.2 \tag{9}$$

These calculations imply that the entrainment rate of the Irminger Current west of Greenland is about 5 times the rate east of Greenland. An immediate interpretation of these

Table 1. The volume transports (per unit height) of the Irminger Current east and west of Greenland and their ratios. See text for details of the two methods used in estimating the mean downstream surface velocities.

$\sqrt{u^2+v^2}$			$u\sin\alpha + v\cos\alpha$		
East (m^2s^{-1})	West (m^2s^{-1})	$\frac{\text{East}}{\text{West}}$	East (m^2s^{-1})	West (m^2s^{-1})	$\frac{\text{East}}{\text{West}}$
$0.20W$	$0.17W$	1.18	$0.19W$	$0.16W$	1.19

results is that due to the more intense exchange with the surrounding, the salinity on the west limb will equal S_0 within 20% of the distance required to achieve it on the east side.

In contrast to the estimate of the ratio q_{east}/q_{west} based on equation (9), the expressions of the fluxes in table 1 imply that estimates of the individual values of q_{east} and q_{west} require the specification of the Current width, W, (in addition to the two individual values of L). In our calculations the current width, W, is determined from the 5-point average of SODA data i.e. a longitudinal span of Current about 100 km near Cape Farewell. Substituting $S_0 = 33.5$ (the bottom-right value in figure 5a), $S_{1,west} = 34.86$ and $S_{1,east} = 34.98$ (these S_1 values are the intercepts of the least square linear lines in the two panels of figure 5) and the values $\partial S/\partial x$ in the two limbs (from the slopes in the two panels of figure 5) in equations (5) yields $L_{east} = 4900$ km and $L_{west} = 850$ km. Physically, these values are the distances that the east and west limbs of the Current have to travel for the salinity of the water they transport to freshen to $S_0 = 33.5$ – the salinity of the surrounding seas. According to equation (6) the combination of these values of L with the flux estimates in table 1 for $W = 100$ km yields entrainment rates of $q_{east} = 0.004\ ms^{-1}$ and $q_{west} = 0.02\ ms^{-1}$.

4 Fresh Water Point-Source Model in the Adriatic Sea

The $S(x)$ structure shown in Figure 6 validates the last approximation in equation (8) since $S(x)$ is nearly constant for $x \geq 0.3x_{end}$.

The parameters S_0, S_{end} and U/κ in the exact $S(x)$ expression are determined by fitting it to the observed salinity distribution along the Sea determined by the averaged (in time and latitude) SODA values (see Section 2). Figure 6 shows the fit between the theoretical least-squared curve (solid curve) and the observed values along the Sea (dots). The theoretical least-squared curve is obtained by substituting $S_0 = 32.6$, $S_{end} = 37.2$ and $U/\kappa = 1.2 \times 10^{-5}\ m^{-1}$ in equation (8). Clearly, this combination of parameter values yields a fit between theory and observations that is as good as can be expected in oceanography. The values of $S_0 = 32.6$ and $S_{end} = 37.2$ are in good agreement with the mean salinity values expected 50 - 100 km from the Po river delta and the Mediterranean Sea, respectively.

An independent check of a combination of these values obtains from the 1^{st}-order term in a Taylor series expansion of $S(x)$ near $x = 0$. Denoting by x_1 the second point from the head of the Sea (recall: the first point is $x = 0$) and approximating $\frac{\partial S}{\partial x}(x = 0) \approx \frac{S(x_1)-S(0)}{x_1}$ where $S(0)$ and $S(x_1)$ are the observed (meridionally averaged) salinities at $x_0 = 0$ and $x_1 = 56,750\ m$, respectively, yields:

$$\frac{U}{\kappa}(S_{end} - S_0) = \frac{\partial S}{\partial x}(x = 0) \approx \frac{S(x_1) - S(0)}{x_1} = 4.3 \times 10^{-5}\ m^{-1}.$$

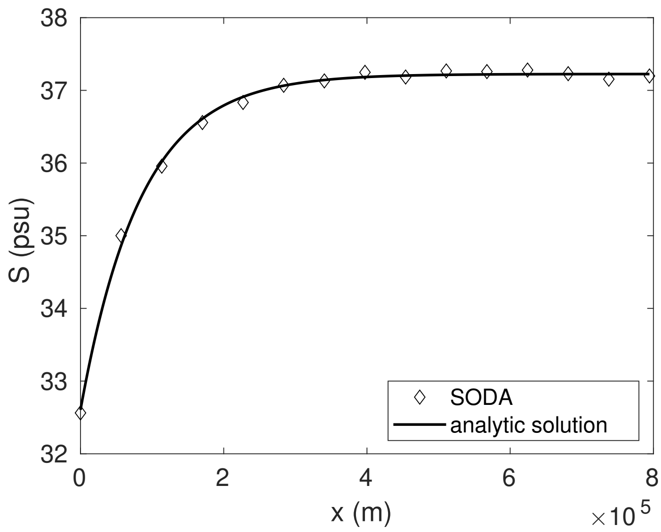

Figure 6. Observed and theoretical variations of salinity along the Adriatic Sea. The distance along the axis of the Adriatic sea is calculated as the linear, planar, distance from the NW point at the head of the Sea: (45.75N,12.25E) denoted as $x = 0$ and the SE point at the strait of Otranto: (40.75N,19.25E) denoted as $x_{end} = 8 \times 10^5$ m.

Since the derivative of $S(x)$ in (8) decays monotonically with x, this estimate of the three parameters compares well with the values $S_0 = 32.6$, $S_{end} = 37.2$ and $U/\kappa = 1.2 \times 10^{-5}\ m^{-1}$ found above from the distribution of $S(x)$ over the entire 800 km Sea.

In conclusion of this section we note that the calculated expression for U/κ implies:

$$\kappa = (8 \times 10^4 m)U, \tag{10}$$

(recall: the units of κ are $m^2 s^{-1}$) which can be used to estimate κ when an estimate of U is available.

5 Summary and Discussion

For over a century, salinity has been used as a simple, yet powerful, diagnostic tool for quantifying horizontal fluxes in and out of semi-enclosed basins that balance the net evaporation from the basin while keeping its salinity and total water volume (i.e. sea level) constant. The present study extends the use of salinity as a diagnostic tool to ocean currents in which the salinity changes downstream. In the Irminger current Where the salinity changes due to entrainment of surrounding fresher water by the current (and detrainment of equal volume of salty water out of the current) the combination of the Freshening Length, which is determined uniquely from SSS variation, and direct transport calculation yields the entrainment rates in two limbs of the Current. Our calculations yield a rate of entrainment that is about 5 times larger in the west limb compared to the east limb. The reanalysis SODA data (both SSS and velocity) yield reliable and robust estimates of the entrainment rates.

In the alternate scenario examined in this study, the downstream changes in salinity are due to the existence of a point-source of fresh water that spreads to the entire Adriatic Sea. In this case the model developed here quantifies the contributions of advection and turbulent exchange to the spreading of fresh water from the source region to the rest of the sea. The comparison is obtained by fitting the steady solution of the advection-diffusion equation to the observed salinity distribution in the basin. In the Adriatic Sea this fit yields a reliable and robust relation between U and κ though neither of these variables can be reliably estimated. The value of the eddy exchange coefficient in Adriatic Sea can thus be evaluated from equation (10) provided U is known. Since its value is fairly small, direct observations of U are subject to large RMS errors so the error in such direct observations exceeds the mean value (see for example Notarstefano et al., 2008). However, estimates of the residence time of drifters in the Sea yield an average value of under 200 days (Poulain & Hariri, 2013). In the 800 km long Sea this residence time implies a mean speed of about 0.04 ms^{-1}. The direct speed estimates in (Notarstefano et al., 2008) set this value to 0.02 ms^{-1}. For an in-between value of $U = 0.03ms^{-1}$ the eddy exchange coefficient in the Adriatic Sea is about 2.5×10^3 m^2s^{-1} and though this value varies linearly with the value assumed for the mean downstream speed, U, its order of magnitude is not expected to change with new estimates of U. The (high) value of κ probably results from the strong gyral circulation in the Sea relative to the weak mean flow.

The use of SSS data for diagnosing ocean currents is of special value when velocity data are highly variable in space or time so direct estimates of transports are subject to large errors. In contrast, SSS data are robust and reliable since stable stratification is ensured in all model calculations and re-analysis data archives. Also, SSS is a standard field reported in all model output and data archives.

This work underscores the potential in using reanalysis climatological SSS fields when direct observations do not provide reliable characterizations of the flow field. The simple and powerful applications of SSS fields in other ocean currents should be explored in future studies as another tool in the Physical Oceanography toolbox that complements the other routinely employed tools. It should also be compared with estimates based on more complex models such as that developed in Lorenz et al. (2021). Future works will extend the ideas developed here to more general circumstances e.g. sub-surface currents in the ocean.

6 Open Research

Only reanalysis SODA data, accessible at https://rda.ucar.edu/datasets/ds650.0/, were used in this study. Only publically available software was used in this study.

Acknowledgments

The authors are pleased to acknowledge that no support was received for this research. We acknowledge helpful discussions with A. D. Kirwan Jr. and Andreas Münchow as well as the comments of three anonymous referees.

References

Artegiani, A., Paschini, E., Russo, A., Bregant, D., Raicich, F., & Pinardi, N. (1997). The adriatic sea general circulation. part i: Air–sea interactions and water mass structure. *Journal of physical oceanography*, *27*(8), 1492–1514.

Berman, H., Paldor, N., Churchill, J., & Lazar, B. (2019). Constraining evaporation rates based on large-scale sea surface transects of salinity or isotopic compositions. *Journal of Geophysical Research: Oceans*, *124*(2), 1322–1330.

Bryden, H. L., & Kinder, T. H. (1991). Steady two-layer exchange through the strait of gibraltar. *Deep Sea Research Part A. Oceanographic Research Papers*, *38*, S445–S463.

Burchard, H., Bolding, K., Feistel, R., Gräwe, U., Klingbeil, K., MacCready, P., ... van der Lee, E. M. (2018). The knudsen theorem and the total exchange flow analysis framework applied to the baltic sea. *Progress in oceanography*, *165*,

268–286.
Carton, J. A., Chepurin, G. A., & Chen, L. (2018). Soda3: A new ocean climate reanalysis. *Journal of Climate*, *31*(17), 6967–6983.
de Jong, M. F., van Aken, H. M., Vage, K., & Pickart, R. S. (2012). Convective mixing in the central Irminger Sea: 2002-2010. *Deep Sea Research Part I: Oceanographic Research Papers*, *63*, 36–51.
Drinkwater, K. F., Sundby, S., & Wiebe, P. H. (2020). Exploring the hydrography of the boreal/arctic domains of North Atlantic seas: Results from the 2013 BASIN survey. *Deep Sea Research Part II: Topical Studies in Oceanography*, *180*, 104880.
Falco, P., Griffa, A., Poulain, P.-M., & Zambianchi, E. (2000). Transport properties in the adriatic sea as deduced from drifter data. *Journal of Physical Oceanography*, *30*(8), 2055 - 2071. Retrieved from `https://journals.ametsoc.org/view/journals/phoc/30/8/1520-0485_2000_030_2055_tpitas_2.0.co_2.xml` doi: 10.1175/1520-0485(2000)030⟨2055:TPITAS⟩2.0.CO;2
Hetland, R. D. (2005). Relating river plume structure to vertical mixing. *Journal of Physical Oceanography*, *35*(9), 1667–1688.
Hetland, R. D. (2010). The effects of mixing and spreading on density in near-field river plumes. *Dynamics of Atmospheres and Oceans*, *49*(1), 37–53.
Knauss, J. A., & Garfield, N. (2016). *Introduction to physical oceanography.* Waveland Press.
Little, C. M., Hu, A., Hughes, C. W., McCarthy, G. D., Piecuch, C. G., Ponte, R. M., & Thomas, M. D. (2019). The relationship between U.S. East Coast sea level and the Atlantic Meridional Overturning Circulation: A review. *J. Geophys. Res. Oceans*, *124*(9), 6435–6458.
Lorenz, M., Klingbeil, K., & Burchard, H. (2021). Impact of evaporation and precipitation on estuarine mixing. *Journal of Physical Oceanography*, *51*(4), 1319–1333.
Notarstefano, G., Poulain, P.-M., & Mauri, E. (2008). Estimation of surface currents in the adriatic sea from sequential infrared satellite images. *Journal of Atmospheric and Oceanic Technology*, *25*(2), 271–285.
Oddo, P., & Guarnieri, A. (2011). A study of the hydrographic conditions in the adriatic sea from numerical modelling and direct observations (2000–2008). *Ocean Science*, *7*(5), 549–567.
Paldor, N., & Anati, D. (1979). Seasonal variations of temperature and salinity in the gulf of elat (aqaba). *Deep Sea Research Part A. Oceanographic Research Papers*, *26*(6), 661–672.
Pickart, R. S., Straneo, F., & Moore, G. (2003). Is Labrador Sea Water formed in the Irminger basin? *Deep Sea Research Part I: Oceanographic Research Papers*, *50*(1), 23–52.
Poulain, P.-M. (1999). Drifter observations of surface circulation in the adriatic sea between december 1994 and march 1996. *Journal of Marine Systems*, *20*(1-4), 231–253.
Poulain, P.-M. (2001). Adriatic sea surface circulation as derived from drifter data between 1990 and 1999. *Journal of Marine Systems*, *29*(1-4), 3–32.
Poulain, P.-M., & Hariri, S. (2013). Transit and residence times in the adriatic sea surface as derived from drifter data and lagrangian numerical simulations. *Ocean Science*, *9*(4), 713–720.
Raicich, F. (1996). On the fresh balance of the adriatic sea. *Journal of Marine Systems*, *9*(3-4), 305–319.
Schmitt, R. W. (1995). The ocean component of the global water cycle. *Reviews of Geophysics*, *33*(S2), 1395–1409.
Sofianos, S. S., & Johns, W. E. (2002). An oceanic general circulation model (ogcm) investigation of the red sea circulation, 1. exchange between the red sea and the indian ocean. *Journal of Geophysical Research: Oceans*, *107*(C11), 17–1.

Wolf-Vecht, A., Paldor, N., & Brenner, S. (1992). Hydrographic indications of advection/convection effects in the gulf of elat. *Deep Sea Research Part A. Oceanographic Research Papers*, *39*(7-8), 1393–1401.